Inorganic Chemistry

Article

pubs.acs.org/IC

Electrochemical and Spectroelectrochemical Studies of Diphosphorylated Metalloporphyrins. Generation of a Phlorin Anion Product

Yuanyuan Fang,[†] Yulia G. Gorbunova,*[,‡,§] Ping Chen,[†] Xiaoqin Jiang,[†] Machima Manowong,[†] Anna A. Sinelshchikova,[‡] Yulia Yu. Enakieva,[‡] Alexander G. Martynov,[‡] Aslan Yu. Tsivadze,[‡,§] Alla Bessmertnykh-Lemeune,[∥] Christine Stern,[∥] Roger Guilard,*[,∥] and Karl M. Kadish*[,†]

[†]Department of Chemistry, University of Houston, Houston, Texas 77204-5003, United States

[‡]Frumkin Institute of Physical Chemistry and Electrochemistry, Russian Academy of Sciences, Leninsky Pr. 31,GSP-1, Moscow, 119071, Russia

[§]Kurnakov Institute of General and Inorganic Chemistry, Russian Academy of Sciences, Leninsky Pr. 31, Moscow, 119991, Russia

[∥]Institut de Chimie Moléculaire de l'Université de Bourgogne, Université de Bourgogne, UMR CRNS n° 6302, 9 Avenue Alain Savary BP 47870, Dijon 21078 CEDEX, France

Supporting Information

ABSTRACT: Two series of diphosphoryl-substituted porphyrins were synthesized and characterized by electrochemistry and spectroelectrochemistry in nonaqueous media containing 0.1 M tetra-*n*-butylammonium perchlorate (TBAP). The investigated compounds are 5,15-bis(diethoxyphosphoryl)-10,20-diphenylporphyrins $(Ph)_2(P(O)(OEt)_2)_2PorM$ and 5,15-bis(diethoxyphosphoryl)-10,20-di(*para*-carbomethoxyphenyl)porphyrins $(PhCOOMe)_2(P(O)(OEt)_2)_2PorM$ where M = 2H, Co(II), Ni(II), Cu(II), Zn(II), Cd(II), or Pd(II). The free-base and five metalated porphyrins with nonredox active centers undergo two ring-centered oxidations and two ring-centered reductions, the latter of which is followed by a chemical reaction of the porphyrin dianion to give an anionic phlorin product. The phlorin anion is electroactive and can be reoxidized by two electrons to give back the starting porphyrin, or it can be reversibly reduced by one electron at more negative potentials to give a phlorin dianion. The chemical conversion of the porphyrin dianion to a phlorin anion proceeds at a rate that varies with the nature of the central metal ion and the solvent. This rate is slowest in the basic solvent pyridine as compared to CH_2Cl_2 and PhCN, giving further evidence for the involvement of protons in the chemical reaction leading to phlorin formation. Calculations of the electronic structure were performed on the Ni(II) porphyrin dianion, and the most favorable atoms for electrophilic attack were determined to be the two phosphorylated carbon atoms. Phlorin formation was not observed after the two-electron reduction of the cobalt porphyrins due to the different oxidation state assignment of the doubly reduced species, a Co(I) π anion radical in one case and an M(II) dianion for all of the other derivatives. Each redox reaction was monitored by thin-layer UV−visible spectroelectrochemistry, and an overall mechanism for each electron transfer is proposed on the basis of these data.

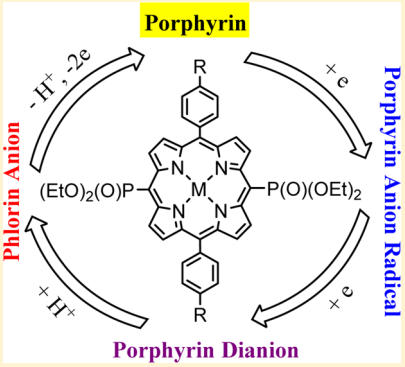

INTRODUCTION

Phosphonate derivatives have been recognized as convenient molecular precursors for functional materials starting from the late 1970s.[1−10] Ongoing research has focused on the development of new scaffolds and design strategies for their assembly.[11,12] Porphyrins are versatile functional molecules in catalysis, light harvesting, and molecular sensing, and they have gained extensive attention in material chemistry. Indeed, structural, photophysical, magnetic, electronic, and catalytic properties of tetrapyrrolic macrocycles are widely used in natural and artificial processes. The assemblage or immobilization of these derivatives provides attractive and simple routes to obtaining advanced functional materials, including catalysts and photo- or electroactive materials.[7,13−17] Early studies on the immobilization of phosphorus-substituted porphyrin derivatives[18−24] have gained a renewed interest after the development of new synthetic approaches toward metalloporphyrins bearing peripheral phosphorus-containing groups at the β-pyrrole and/or the *meso* positions of the porphyrin macrocycle.[25−27] Moreover, phosphonate diesters were recently recognized as important molecular building blocks to mimic the natural photosynthesis process and to construct coordination polymers.[28−44]

Along these lines, it is important to gain insight into the electrochemical behavior of these porphyrins due to the

Received: January 9, 2015
Published: March 19, 2015

DOI: 10.1021/acs.inorgchem.5b00067
Inorg. Chem. 2015, 54, 3501−3512

Chart 1. Investigated Porphyrins

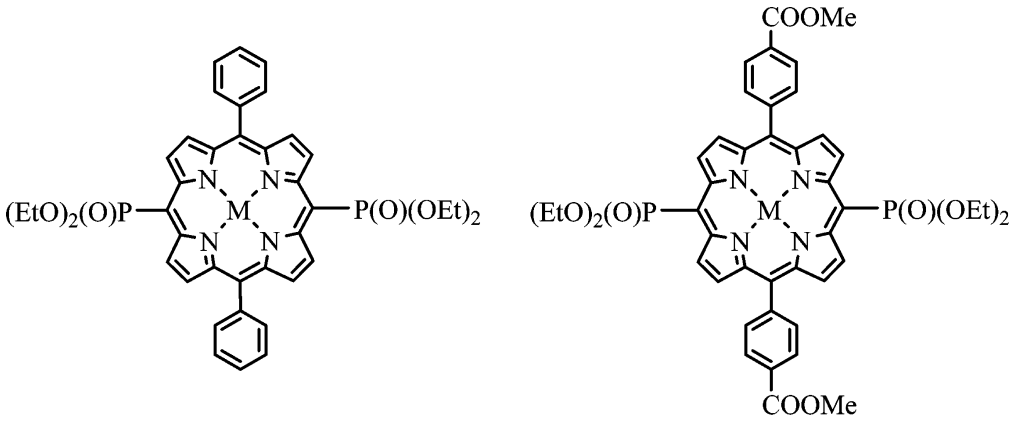

1M **2M**

M = H_2, Ni(II), Cu(II), Pd(II), Zn(II), Cd(II), Co(II)

importance of electron-transfer processes for catalytic and photochemical studies of supramolecular architectures and hybrid functional materials.[28]

Despite the large interest in phosphorylated porphyrins, only a few studies have been dedicated to elucidating, in detail, the electrochemical and spectroelectrochemical properties of porphyrins containing $P(O)(OR)_2$ at a peripheral position of the macrocycle where R is an alkyl group.[29−32] An initial study on the electrochemistry of *meso*-diphosphoryl porphyrins showed the unexpected presence of three reductions,[29,30] but only the first was characterized; no spectroscopic measurements were made on the electroreduction products, which would be needed for a mechanistic characterization of the reactions that occurred in solution following electron transfer. This is addressed in the current manuscript, which expands upon the number of examined compounds and reports the electrochemistry and spectroelectrochemistry of two series of *meso*-bis(diethoxyphosphoryl)porphyrins in three nonaqueous solvents (see Chart 1). One aim of this study is to characterize electrochemistry of the *meso* substituted phosphoryl porphyrins, while another is to examine how the nature of the central metal ion, solvent, and/or the site of electron transfer will influence the electronic properties and oxidation/reduction mechanisms of these compounds.

EXPERIMENTAL SECTION

Materials. Unless otherwise noted, all chemicals and starting materials were obtained commercially from Acros and Sigma-Aldrich Co. and used without further purification. Chloroform and methanol were freshly distilled before use. Silica gel 60 (0.063−0.20 mm, 70−230 mesh ASTM, Merck) and aluminum oxide (0.063−0.20 mm, basic, activated Brockmann II−III, Merck) were used for column chromatography. Dichloromethane (CH_2Cl_2, 99.8%, EMD Chemicals Inc.) and pyridine (Py, Sigma-Aldrich Co.) were used as received. Benzonitrile (PhCN) was purchased from Sigma-Aldrich Co. and freshly distilled over P_2O_5 before use. Tetra-*n*-butylammonium perchlorate (TBAP) was purchased from Sigma-Aldrich Co. ***Caution!*** *Perchlorate salts are potentially explosive and should be handled with care.*

All synthesis reactions were performed in oven-dried glassware under a slight positive pressure of argon. Analytical thin-layer chromatography (TLC) was carried out using Merck silica gel 60 plates (precoated sheets, 0.2 mm thick, with fluorescence indicator F254).

Instrumentation. Cyclic voltammetry was performed at 298 K using an EG&G Princeton Applied Research (PAR) 173 potentiostat/galvanostat. A homemade three-electrode cell was used for cyclic voltammetric measurements and consisted of a glassy carbon working electrode, a platinum counter electrode, and a homemade saturated calomel reference electrode (SCE). The SCE was separated from the bulk of the solution by a fritted glass bridge of low porosity, which contained the solvent/supporting electrolyte mixture.

UV−visible spectra of the neutral compounds were measured on a Varian Cary 100 spectrophotometer, while spectra of the oxidized or reduced species were obtained with a Hewlett-Packard 8453 diode array spectrophotometer. Thin-layer UV−visible spectroelectrochemical experiments were performed using a home-built thin-layer cell, which has a transparent platinum net working electrode. Potentials were applied and monitored with an EG&G PAR Model 173 potentiostat. High-purity N_2 from Trigas was used to deoxygenate the solution and kept over the solution during each electrochemical and spectroelectrochemical experiment.

^1H and ^{31}P NMR spectra were recorded on Bruker Avance 300 III NanoBay and Avance 600 spectrometers. All chemical shifts are given in parts per million, referenced on the δ scale using a residual solvent peak as internal standard for ^1H and phosphoric acid (H_3PO_4) as an external standard for the ^{31}P NMR data. Coupling constants are given in hertz. Mass spectra were obtained in linear mode with a Bruker Proflex III MALDI-TOF mass spectrometer without matrix and accurate mass measurements (high-resolution mass spectrometry (HRMS)) using a Orbitrap ESI-TOF mass spectrometer. IR spectra were registered on a Fourier transform infrared (FT-IR) Nexus (Nicolet) spectrometer using micro-ATR accessory (Pike). HRMS and FT-IR measurements were made at the "Pôle Chimie Moléculaire", the technological platform for chemical analysis and molecular synthesis (http://www.wpcm.fr), which relies on the Institute of the Molecular Chemistry of University of Burgundy and Welience, a Burgundy University private subsidiary.

Computational Details. Geometry optimization and normal-mode frequency analysis were performed with SPARTAN'14 software (Wave function Inc.), using 6-31G* basis set[45−48] and B3LYP functional.[49,50] Graphical analysis of electronic density was performed with CHEMSIISAN 4.33 software (http://www.chemissian.com/). ZINDO/s calculations of UV−vis spectra were performed with ORCA 2.9.1 software.[51]

Synthesis. 5,15-bis(diethoxyphosphoryl)-10,20-diphenylporphyrin (**1H$_2$**) and its zinc(II) or copper(II) complexes (**1Zn**) and (**1Cu**) were synthesized according to literature procedures.[29,30,33]

Cadmium(II) 5,15-Bis(diethoxyphosphoryl)-10,20-diphenylporphyrinate (1Cd). A solution of porphyrin **1H$_2$** (15.6 mg, 2.12×10^{-2} mmol), cadmium acetate (19.6 mg, 8.50×10^{-2} mmol), and

DOI: 10.1021/acs.inorgchem.5b00067
Inorg. Chem. 2015, 54, 3501−3512

$NaHCO_3$ (28.2 mg, 0.336 mmol) in chloroform−methanol mixture (2.85 mL, 9/1 v/v) was stirred at room temperature for 1.5 h. The volatiles were removed in vacuo. A green residue was purified by column chromatography on basic alumina using a mixture of $CHCl_3$/MeOH (99/1 v/v) as an eluent. Complex **1Cd** was obtained as a green solid (17.2 mg, 96%). ^{1}H NMR (300 MHz, $CDCl_3/CD_3OD$, 2/1 v/v, 25 °C): δ 1.17 (t, J = 7.0 Hz, 12H, CH_3), 4.07−3.97 (m, 4H, CH_2O), 4.33−4.20 (m, 4H, CH_2O), 7.59 (m, 6H, *m*-,*p*-Ph), 7.96 (d, J = 7.4 Hz, 4H, *o*-Ph), 8.56 (d, J = 4.7 Hz, 4H, β-H), 9.88 (d, J = 4.7 Hz, 4H, β-H) ppm. ^{31}P NMR ($CDCl_3/CD_3OD$, 2/1 v/v, 121 MHz, 25 °C): δ 25.4 ppm. FT-IR (ν_{max}, cm^{-1}): 2916(w), 2850(w), 1595(w), 1508(m), 1438(m), 1382(m), 1226(s), 1196(s), 1083(m), 1075(m), 1033(m), 983(m), 950(s), 885(s), 802(m), 754(m),730(m), 700(m), 665(m). UV−vis ($CHCl_3$, λ_{max}, nm (log(ε)): 430 (5.26), 572 (3.92), 610 (4.28). HRMS: m/z $[M + Na]^+$ calcd for $C_{40}H_{38}N_4CdO_6P_2Na$: 869.12035, found: 869.11603.

Nickel(II) 5,15-Bis(diethoxyphosphoryl)-10,20-diphenylporphyrinate (1Ni). Method A. The porphyrin $\mathbf{1H_2}$ (10.0 mg, 1.36×10^{-2} mmol) and nickel(II) acetylacetonate (14.0 mg, 5.45×10^{-2} mmol) were dissolved in 2.5 mL of 1,2-dichlorobenzene, and the mixture stirred at reflux for 5 min. After it cooled, the reaction mixture was evaporated in vacuo. The violet residue was dissolved in $CHCl_3$ and purified by column chromatography on silica gel using hexane/$CHCl_3$ (15/85 v/v) as an eluent. Complex **1Ni** was isolated as a violet solid after evaporation of the solvents in vacuo (10.6 mg, yield 99%). **Method B**. The porphyrin $\mathbf{1H_2}$ (10.0 mg, 1.36×10^{-2} mmol) and nickel(II) acetate (9.6 mg, 5.43×10^{-2} mmol) were dissolved in 2 mL of 1,2-dichlorobenzene. The reaction mixture was stirred at reflux for 45 min. The solvent was removed under reduced pressure. The violet residue was dissolved in $CHCl_3$ and purified by column chromatography on silica gel using hexane/$CHCl_3$ (15/85 v/v). Compound **1Ni** was isolated as a violet solid after evaporation of solvents in vacuo (9.3 mg, yield 87%). ^{1}H NMR ($CDCl_3/CD_3OD$, 2/1 v/v, 300 MHz, 25 °C): δ 1.14 (t, J = 7.1 Hz, 12H, CH_3), 4.03−3.87 (m, 4H, CH_2O), 4.16−4.07 (m, 4H, CH_2O), 7.50 (m, 6H, *m*-,*p*-Ph), 7.72 (d, J = 7.6 Hz, 4H, *o*-Ph), 8.52 (d, J = 5.1 Hz, 4H, β-H), 9.62 (d, J = 5.2 Hz, 4H, β-H) ppm. ^{31}P NMR ($CDCl_3/CD_3OD$, 2/1 v/v, 121 MHz, 25 °C): δ 19.6 ppm. FT-IR (ν_{max}, cm^{-1}): 2980(w), 2900(w), 1600(w), 1535(m), 1436(m), 1390(m), 1348(m), 1253(s), 1203(m), 1158(m), 1092(m), 1013(s), 963(s), 888(s), 808(m), 750(s), 696(m), 663(m). UV−vis ($CHCl_3$, λ_{max}, nm, log(ε)): 417 (5.22), 553 (3.92), 597 (4.32). HRMS: m/z $[M]^+$ calcd for $C_{40}H_{38}N_4NiO_6P_2$: 790.16146, found: 790.15959; $[M + H]^+$ calcd for $C_{40}H_{39}N_4NiO_6P_2$: 791.16928, found: 791.16544; $[M + Na]^+$ calcd for $C_{40}H_{38}N_4NiO_6P_2Na$: 813.15123, found: 813.14623.

Palladium(II) 5,15-Bis(diethoxyphosphoryl)-10,20-diphenylporphyrinate (1Pd). The palladium(II) acetate (14.4 mg, 6.41×10^{-2} mmol) was added to a solution of $\mathbf{1H_2}$ (11.8 mg, 1.6×10^{-2} mmol) in $CHCl_3$ (3 mL). The reaction mixture was stirred at reflux for 10 min. After this mixture cooled, the volatiles were evaporated under reduced pressure. A pink residue was dissolved in $CHCl_3$ and purified by column chromatography on silica gel using hexane/$CHCl_3$ (40/60 v/v) as an eluent. The product was obtained as a pink solid **1Pd** (13.0 mg, 97%). ^{1}H NMR ($CDCl_3$, 300 MHz, 25 °C): δ 1.35 (t, J = 7.0 Hz, 12H, CH_3), 4.28−4.15 (m, 4H, CH_2O), 4.56−4.43 (m, 4H, CH_2O), 7.83−7.73 (m, 6H, *m*-,*p*-Ph), 8.11 (d, J = 7.0 Hz, 4H, *o*-Ph), 8.86 (d, J = 5.2 Hz, 4H, β-H), 10.32 (d, J = 5.2 Hz, 4H, β-H) ppm. ^{31}P NMR ($CDCl_3$,121 MHz, 25 °C): δ 21.0 ppm. FT-IR (ν_{max}, cm^{-1}): 2975(w), 2926(w), 1600(w), 1543(m), 1431(m), 1390(m), 1348(m), 1251(s), 1203(m), 1151(w), 1092(m), 1000(m), 950(s), 883(s), 802(s), 750(s), 702(s), 665(m). UV−vis ($CHCl_3$, λ_{max}, nm, log(ε)): 412 (5.54), 538 (4.28), 597 (4.77). HRMS: m/z $[M + H]^+$ calcd for $C_{40}H_{39}N_4PdO_6P_2$: 839.13889, found: 839.13525; $[M + Na]^+$ calcd for $C_{40}H_{38}N_4PdO_6P_2Na$: 861.12083, found: 861.11766.

Cobalt(II) 5,15-Bis(diethoxyphosphoryl)-10,20-diphenylporphyrinate (1Co). The porphyrin $\mathbf{1H_2}$ (30.4 mg, 4.1×10^{-2} mmol) and cobalt(II) acetate (41.2 mg, 0.165 mmol) were dissolved in a mixture of $CHCl_3$ (6 mL) and CH_3OH (0.65 mL). The reaction mixture was stirred at reflux for 1 h. After this mixture cooled, the volatiles were removed under reduced pressure. The residue was dissolved in $CHCl_3$ and purified by column chromatography on silica gel using $CHCl_3$ as an eluent. Compound **1Co** was isolated as a green solid (32.7 mg, yield 99%). FT-IR (ν_{max}, cm^{-1}): 2978(w), 2890(w), 1600(w), 1534(m), 1388(m), 1366(m), 1346(m), 1245(s), 1203(m), 1160(m), 1075(m), 1041(m), 1014(vs), 992(m), 950(s), 885(s), 795(s), 750(s),732(m), 700(s), 6658(m). UV−vis ($CHCl_3$, λ_{max}, nm, log(ε)): 411 (5.09), 550 (3.84), 590 (4.13). HRMS: m/z $[M + H]^+$ calcd for $C_{40}H_{39}N_4CoO_6P_2$: 792.16768, found: 792.16525; $[M + Na]^+$ calcd for $C_{40}H_{38}N_4CoO_6P_2Na$: 814.14963, found: 814.14766.

5,15-Bis(diethoxyphosphoryl)-10,20-di(*para*-carbomethoxyphenyl)porphyrin ($\mathbf{2H_2}$). The same procedure as for $\mathbf{1H_2}$ was applied and yielded $\mathbf{2H_2}$ as violet solid in 86% yield. ^{1}H NMR ($CDCl_3/CD_3OD$, 5/2 v/v, 600 MHz, 25 °C): δ 1.38 (t, J = 7.0 Hz, 12H, CH_3), 4.59−4.20 (m, 8H, CH_2O), 4.16 (s, 6H, OCH_3), 8.30 (d, J = 7.0 Hz, 4H, *m*-Ph), 8.50 (d, J = 7.0 Hz, 4H, *o*-Ph), 8.85 (d, J = 7.0 Hz, 4H, β-H), 10.27 (d, J = 7.0 Hz, 4H, β-H) ppm. ^{31}P NMR ($CDCl_3$, 121 MHz, 25 °C): δ 21.2 ppm. FT-IR (ν_{max}, cm^{-1}): 3280(w), 3160(w), 2985(w), 2950(w), 1720(s), 1716(s), 1606(m), 1557(m), 1553(m), 1432(m), 1390(m), 1335(m), 1313(w), 1275(vs), 1249(vs), 1212(s), 1190(m), 1165(m), 1142(m), 1110(m), 1098(m), 1067(m), 1034(m), 1012(vs), 950(s), 930(s), 883(s), 818(s), 795(s), 790(s), 760(s), 745(s), 732(s), 707(m), 667(m), 633(m). UV−vis ($CHCl_3$, λ_{max}, nm, log(ε)): 418 (5.40), 520 (4.32), 558 (4.38), 596 (4.18), 650 (4.33). HRMS: m/z $[M + H]^+$ calcd for $C_{44}H_{45}N_4O_{10}P_2$: 851.26054, found: 851.26263; $[M + Na]^+$ calcd for $C_{44}H_{44}N_4O_{10}P_2Na$: 873.24249, found: 873.24053.

Zinc(II) 5,15-Bis(diethoxyphosphoryl)-10,20-di(*para*-carbomethoxyphenyl)-porphyrin (2Zn). A solution of $\mathbf{2H_2}$ (63.7 mg, 7.49×10^{-2} mmol) and zinc(II) acetate (82 mg, 0.375 mmol) in a mixture of dichloromethane (20 mL) and methanol (1 mL) was stirred at room temperature overnight. Solvents were removed under reduced pressure. A green residue was purified by column chromatography on silica gel using CH_2Cl_2/MeOH (99/1 v/v) as eluent. Complex **2Zn** was obtained as a green solid (64.4 mg, 94%). ^{1}H NMR (600 MHz, $CDCl_3/CD_3OD$, 5/2 v/v, 25 °C): δ 1.17 (t, J = 7.1 Hz, 12H, CH_3), 3.93 (s, 6H, OCH_3), 4.12−3.99 (m, 4H, CH_2O), 4.35−4.25 (m, 4H, CH_2O), 8.05 (d, J = 8.0 Hz, 4H, *m*-Ph), 8.23 (d, J = 8.0 Hz, 4H, *o*-Ph), 8.6 (d, J = 4.9 Hz, 4H, β-H), 10.06 (d, J = 4.9 Hz, 4H, β-H) ppm. ^{31}P NMR ($CDCl_3/CD_3OD$, 5/2 v/v, 121 MHz, 25 °C): δ 27.17 ppm. FT-IR (ν_{max}, cm^{-1}): 2980(w), 2950(w), 1720(vs), 1607(m), 1528(m), 1437(m), 1400(m), 1388(m), 1274(vs), 1245(m), 1230(w), 1200(m), 1162(m), 1112(m), 1098(m), 1040(m), 1010(vs), 983(s), 950(s), 891(s), 863(s), 800(s), 762(s), 740(s), 713(m), 706(m), 668(m), 636(m). UV−vis ($CHCl_3$, λ_{max}, nm (log(ε)): 426 (5.51), 563 (4.01), 603 (4.37). HRMS: m/z $[M]^+$ calcd for $C_{44}H_{42}N_4O_{10}P_2Zn$: 912.17254, found: 912.16621; $[M + H]^+$ calcd for $C_{44}H_{43}N_4O_{10}P_2Zn$: 913.17459, found: 913.17812; $[M + Na]^+$ calcd for $C_{44}H_{42}N_4O_{10}P_2ZnNa$: 935.15598, found: 935.15910.

Copper(II) 5,15-Bis(diethoxyphosphoryl)-10,20-di(*para*-carbomethoxyphenyl)-porphyrinate (2Cu). A solution of $\mathbf{2H_2}$ (30.2 mg, 3.5×10^{-2} mmol) in a mixture of $CHCl_3$ (5 mL) and CH_3OH (0.5 mL) and copper(II) acetate (25.7 mg, 0.142 mmol) was stirred at room temperature for 50 min. Solvents were removed under reduced pressure. The blue−violet residue was dissolved in $CHCl_3$ and purified by column chromatography on silica gel using hexane/$CHCl_3$ (10/90 v/v). Compound **2Cu** was isolated as a blue−violet solid (31.6 mg, yield 99%). FT-IR (ν_{max}, cm^{-1}): 2980(w), 2926(w), 1730(s), 1720(vs), 1608(m), 1535(m), 1440(m), 1400(m), 1276(vs), 1247(s), 1230(w), 1205(m), 1190(m), 1180(m), 1158(m), 1114(m), 1110(m), 1088(m), 1064(m), 1035(m), 1010(vs), 990(s), 965(s), 950(s), 892(s), 867(s), 822(m), 800(s), 762(s), 737(s), 732(m), 709(s), 667(m), 663(m). UV−vis ($CHCl_3$, λ_{max}, nm (log(ε)): 417 (5.42), 552 (4.18), 595 (4.43). HRMS: m/z $[M + H]^+$ calcd for $C_{44}H_{43}N_4O_{10}P_2Cu$: 912.17449, found: 912.17756; $[M + Na]^+$ calcd for $C_{44}H_{42}N_4O_{10}P_2CuNa$: 934.15644, found: 934.15673.

Cadmium(II) 5,15-Bis(diethoxyphosphoryl)-10,20-di(*para*-carbomethoxyphenyl)-porphyrinate (2Cd). A solution of porphyrin $\mathbf{2H_2}$ (13.4 mg, 1.6×10^{-2} mmol), cadmium acetate (14.5 mg, 6.4×10^{-2} mmol), and $NaHCO_3$ (21.2 mg, 0.252 mmol) in chloroform−methanol mixture (2.15 mL, 9/1 v/v) was stirred at room

DOI: 10.1021/acs.inorgchem.5b00067
Inorg. Chem. 2015, 54, 3501−3512

Table 1. Half-Wave Potentials (V vs SCE) for Ring-Centered Redox Reactions of Investigated Compounds in PhCN, Containing 0.1 M TBAP

		oxidation		reduction				
compound	M	second	first	first	second	third[a]	H–L Gap	ref
$(Ph)_2(P(O)(OEt)_2)_2$PorM **1**	2H	1.28	1.28	−0.77	−1.28	−1.70	2.05	29
	Ni	1.33	1.25	−0.83	−1.40	−1.76	2.08	this work (tw)
	Cu	1.36	1.22	−0.86	−1.43[b]	−1.73	2.08	29
	Pd	1.76[b]	1.32	−0.90	−1.49[b]	−1.81	2.22	tw
	Zn	1.32[b]	1.06	−0.97	−1.42[b]		2.03	29
	Cd	1.45[b]	1.05	−1.13	−1.43	−1.88[b]	2.18	tw
$(PhCOOMe)_2(P(O)(OEt)_2)_2$PorM **2**	2H	1.36	1.36	−0.68	−1.20	−1.52	2.04	tw
	Ni	1.30	1.30	−0.81	−1.36	−1.64	2.11	tw
	Cu	1.36	1.22	−0.82	−1.34	−1.60[c]	2.04	tw
	Zn	1.24	1.10	−0.96	−1.40[b]	−1.79	2.06	tw
	Cd	1.14	1.14	−0.89	−1.32[b]	−1.79	2.03	tw
(TPP)M **3**	2H	1.35	1.05	−1.19	−1.53		2.24	52
	Ni	1.13	1.02	−1.26	−1.75		2.28	53
	Cu	1.33	0.99	−1.28	−1.74		2.27	54
	Pd	1.53	1.15	−1.25	−1.75		2.40	tw
	Zn	1.14	0.82	−1.32	−1.74		2.14	55
	Cd		0.72	−1.34			2.06	56

[a]Reduction of phlorin anion generated in solution after second electron addition. [b]Irreversible peak potential at scan rate = 0.1 V/s. [c]Additional peak observed at $E_{1/2}$ = −1.76 V.

temperature for 2.5 h. Solvents were removed under reduced pressure. A green residue was purified by column chromatography on basic alumina using a mixture of $CHCl_3$/MeOH (98.5/1.5% v/v) as eluent. Complex **2Cd** was obtained as a green solid (14.3 mg, 95%). ^{1}H NMR (600 MHz, $CDCl_3/CD_3OD$, 2/1 v/v, 25 °C): δ 1.18 (t, J = 7.1 Hz, 12H, CH_3), 3.97 (s, 6H, OCH_3), 4.01–4.11 (m, 4H, CH_2O), 4.20–4.33 (m, 4H, CH_2O), 8.08 (d, J = 8.0 Hz, 4H, *m*-Ph), 8.26 (d, J = 8.0 Hz, 4H, *o*-Ph), 8.52 (d, J = 4.7 Hz, 4H, β-H), 9.91 (d, J = 4.7 Hz, 4H, β-H) ppm. ^{31}P NMR ($CDCl_3/CD_3OD$, 2/1 v/v, 121 MHz, 25 °C): δ 27.17 ppm. FT-IR (ν_{max}, cm^{-1}): 2985(w), 2945(w), 1720(vs), 1606(m), 1520(m), 1435(m), 1390(m), 1273(vs), 1249(m), 1205(w), 1190(m), 1160(m), 1112(m), 1100(m), 1038(m), 1010(vs), 980(s), 965(s), 940(s), 891(s), 862(s), 794(s), 762(s), 740(s), 711(s), 667(m), 635(m). UV–vis ($CHCl_3$, λ_{max}, nm (log(ε)): 432 (5.24), 574 (3.95), 611 (4.23). HRMS: m/z $[M + H]^+$ calcd for $C_{44}H_{43}N_4O_{10}P_2Cd$: 963,14880, found: 963.14456; $[M + Na]^+$ calcd for $C_{44}H_{42}N_4O_{10}P_2CdNa$: 985.13074, found: 985.13273.

Cobalt(II) 5,15-Bis(diethoxyphosphoryl)-10,20-di(*para*-carbomethoxyphenyl)-porphyrinate (2Co). A solution of porphyrin $\mathbf{2H_2}$ (31.4 mg, 3.7×10^{-2} mmol) and cobalt(II) acetate (36.8 mg, 0.148 mmol) in a mixture of chloroform (6.5 mL) and methanol (0.65 mL) was stirred at reflux for 1.5 h at nitrogen atmosphere. Solvents were removed under reduced pressure. The product was isolated by column chromatography on silica gel using $CHCl_3$/MeOH (98/2 v/v) giving **2Co** as a green solid (27.8 mg, yield 83%). FT-IR (ν_{max}, cm^{-1}): 2921(w), 2850(w), 1720(vs), 1608(m), 1538(m), 1435(m), 1390(m), 1345(w), 1274(s), 1250(w), 1200(m), 1160(m), 1112(m), 1100(m), 1040(m), 1014(vs), 960(s), 894(s), 864(s), 818(m), 794(s), 765(s), 735(s), 707(s), 668(m), 637(m). UV–vis ($CHCl_3$, λ_{max}, nm, log(ε)): 411 (5.04), 549 (3.94), 590 (4.28). HRMS: m/z $[M]^+$ calcd for $C_{44}H_{42}N_4O_{10}P_2Co$: 907.17027, found: 907.17377.

Nickel(II) 5,15-Bis(diethoxyphosphoryl)-10,20-di(*para*-carbomethoxyphenyl)-porphyrinate (2Ni). The nickel(II) acetylacetonate (12.6 mg, 4.8×10^{-2} mmol) was added to a solution of porphyrins $\mathbf{2H_2}$ (10.4 mg, 1.2×10^{-2} mmol) in 1,2-dichlorobenzene (5 mL). The reaction mixture was stirred at reflux for 5 min. Solvents were removed under reduced pressure. The red–violet residue was dissolved in $CHCl_3$ and purified by column chromatography on silica gel using $CHCl_3$ as an eluent. Complex **2Ni** was isolated as a red–violet solid (10.9 mg, yield 97%). ^{1}H NMR ($CDCl_3$, 600 MHz, 25 °C): δ 1.34 (t, J = 7.0 Hz, 12H, CH_3), 4.09 (s, 6H, OCH_3), 4.12–4.21 (m, 4H, CH_2O), 4.34–4.44 (m, 4H, CH_2O), 8.01 (d, J = 7.8 Hz, 4H, *m*-Ph), 8.36 (d, J = 7.8 Hz, 4H, *o*-Ph), 8.65 (d, J = 5.0 Hz, 4H, β-H), 9.96 (d, J = 5.0 Hz, 4H, β-H) ppm. ^{31}P NMR ($CDCl_3$, 121 MHz, 25 °C): δ 19.13 ppm. FT-IR (ν_{max}, cm^{-1}): 2983(w), 2952(w), 1722(vs), 1608(m), 1540(m), 1436(m), 1400(m), 1348(m), 1274(vs), 1253(s), 1206(m), 1190(m), 1180(m), 1163(m), 1112(m), 1100(m), 1043(m), 1016(vs), 1002(m), 963(s), 895(s), 865(s), 820(m), 800(s), 765(s), 736(m), 710(s), 668(m). UV–vis ($CHCl_3$, λ_{max}, nm, log(ε)): 419 (5.24), 552 (4.19), 597 (4.44). HRMS: m/z $[M]^+$ calcd for $C_{44}H_{42}N_4O_{10}P_2Ni$: 906.17242, found: 906.17687; $[M + H]^+$ calcd for $C_{44}H_{43}N_4O_{10}P_2Ni$: 907.18024, found: 907.18065; $[M + Na]^+$ calcd for $C_{44}H_{42}N_4O_{10}P_2NiNa$: 929.16273, found: 929.16184.

RESULTS AND DISCUSSION

Synthesis. 5,15-Bis(diethoxyphosphoryl)-10,20-diphenylporphyrin $\mathbf{1H_2}$ and 5,15-bis(diethoxyphosphoryl)-10,20-di(*para*-carbomethoxyphenyl)porphyrin $\mathbf{2H_2}$ were obtained according to the Hirao reaction.[33] Metalation was performed using the traditional porphyrin coordination chemistry approach and consisted of reacting the free-base porphyrin with acetates of the target metal ion. As expected, experimental conditions for metalation of the free-base porphyrins were dependent on the nature of the metal ion. A quantitative metalation could be achieved by treatment of $\mathbf{1H_2}$ or $\mathbf{2H_2}$ with an excess of copper(II), zinc(II), or cadmium(II) acetate in a chloroform/methanol solution at room temperature. The palladium(II) and cobalt(II) complexes were prepared in quantitative yield by reacting $\mathbf{1H_2}$ and $\mathbf{2H_2}$ with the metal(II) acetates in $CHCl_3$ at reflux. Nickel(II) acetate and nickel(II) acetylacetonate were found to be suitable precursors for synthesis of the nickel porphyrins in high yield, and the metal insertion reactions proceeded smoothly in 1,2-dichlorobenzene at reflux.

Electrochemistry. The electrochemical properties of each compound were studied by cyclic voltammetry in three nonaqueous solvents (PhCN, CH_2Cl_2, and pyridine) containing TBAP as supporting electrolyte. Half-wave potentials for oxidation and reduction in each solvent are given in Tables 1 (PhCN) and 2 (Py) as well as in Supporting Information, Table

DOI: 10.1021/acs.inorgchem.5b00067
Inorg. Chem. 2015, 54, 3501–3512

Table 2. Half-Wave Potentials (V vs SCE) of Investigated Compounds with Redox Inactive Metal Centers in Py, Containing 0.1 M TBAP

		reduction		
compound	M	first	second	third[a]
$(Ph)_2(P(O)(OEt)_2)_2$Por **1**	2H	−0.79	−1.33	
	Ni	−0.91	−1.48	−1.84
	Cu	−0.95	−1.47	−1.79
	Pd	−0.88	−1.45	−1.81
	Cd	−0.98	−1.55	−1.96
	Zn	−0.97	−1.53	−1.94
$(PhCOOMe)_2(P(O)(OEt)_2)_2$Por **2**	2H	−0.74	−1.27	
	Ni	−0.91	−1.44	−1.72
	Cu	−0.91	−1.41	−1.68
	Zn	−1.02	−1.59	−1.99
	Cd	−0.94	−1.48	−1.96[b]

[a]Reduction of phlorin anion generated in solution after second electron addition. [b]Additional peak observed at $E_{1/2}$ = −1.79 V.

S1 (CH_2Cl_2), and the electrochemical properties are discussed below, first for the porphyrins with redox inactive central metal ions and then for the cobalt(II) derivatives, which undergo oxidation and reduction at the metal center to give derivatives of Co(III) and Co(I).

Porphyrins with Redox-Inactive Metal Centers. Phlorin Anion Generation. Similar redox behavior is observed for the H_2, Cu^{II}, Ni^{II}, Cd^{II}, Zn^{II}, and Pd^{II} porphyrins (**1M** and **2M**) in PhCN and CH_2Cl_2. These porphyrins with electroinactive metal centers undergo four ring-centered processes to give π-cation radicals and dications upon oxidation and π-anion radicals and dianions upon reduction. However, the second one-electron reduction results in formation of a porphyrin dianion and is followed by a fast chemical reaction providing a species that can be reoxidized to give back the starting porphyrin or can be reversibly reduced by one electron at more negative potentials.

An illustration of the chemical reaction involving the doubly reduced porphyrins is given by the series of cyclic voltammograms in Figure 1 for **1Pd** in PhCN and pyridine. Three reductions are observed in PhCN between 0.0 and −2.00 V versus SCE. All three redox processes have similar cathodic peak currents, indicating the same number of electrons transferred in each step. The first reduction, at $E_{1/2}$ = −0.90 V, is reversible when switching the direction of the potential sweep at −1.20 V (top CV in Figure 1a), and the third reduction at $E_{1/2}$ = −1.81 V is also reversible in PhCN when scanning to −2.00 V (third CV in Figure 1a). This contrasts with the reduction of **1Pd** at E_{pc} = −1.49 V, which has a shape consistent with a reversible one-electron addition ($E_{pc} - E_{p/2}$ = 60 mV) on the forward scan and the lack of a coupled anodic peak on the reverse sweep. This can be related with the chemical reaction to give a product that undergoes an irreversible oxidation at E_{pc} = −0.13 V and a reversible reduction at $E_{1/2}$ = −1.81 V in PhCN.

We suspected that the product of the homogeneous chemical reaction involved protonation of the doubly reduced species and phlorin anion formation as earlier reported in the literature for Zn(II) and free-base tetraphenylporphyrins (TPP), which were chemically converted to a phlorin anion at the electrode surface after generation of the porphyrin dianion in dimethylformamide (DMF).[34,35] To prove this hypothesis, we switched to pyridine as a basic solvent. The cyclic voltammogram for **1Pd** under this solution condition is shown in Figure 1b where the second reduction has become almost reversible, while the currents for the processes at $E_{1/2}$ = −1.81 and E_p = −0.13 V are both significantly reduced in intensity, as compared to what is seen in PhCN (Figure 1a). A comparison of the electrochemistry for **1Pd** in PhCN and pyridine further suggests that the chemical reaction of the electrogenerated dianion involves protonation, which would be minimized in the basic solvent, leading to a slower rate of the chemical reaction and decreasing current for the third reduction.

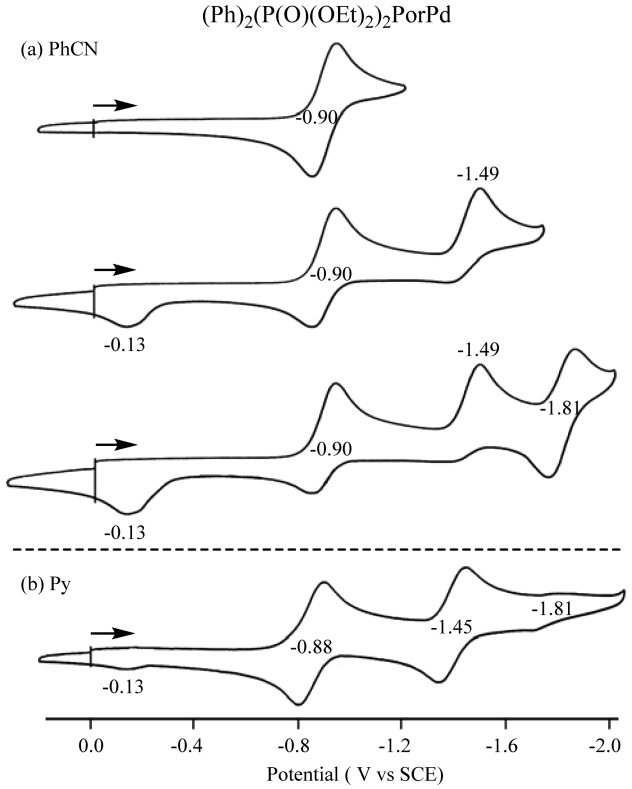

Figure 1. Cyclic voltammograms of $(Ph)_2(P(O)(OEt)_2)_2$PorPd in (a) PhCN and (b) pyridine containing 0.1 M TBAP. Scan rate = 0.1 V/s.

Similar solvent-dependent redox behavior is seen for the H_2, Cu^{II}, and Ni^{II} porphyrins as shown in Figure 2, where the currents for the third reduction at $E_{1/2}$ = −1.52 to −1.79 V in PhCN are significantly decreased in intensity when the measurement is performed in the basic solvent pyridine. However, a different behavior is observed for the Zn^{II} porphyrin in pyridine where the third reduction remains well-defined, suggesting that the chemical reaction following formation of the porphyrin dianion varies not only with the solvent but also with the nature of the central metal ion.

Cyclic voltammograms for reduction of the porphyrins with nonredox-active central metal ions in CH_2Cl_2, 0.1 M TBAP are similar to those in PhCN, and an example of this is illustrated in Supporting Information, Figure S1 for **1Zn** and **1Cd**. The current−voltage curves are well-defined for both porphyrins in CH_2Cl_2, and the measured half-wave or peak potentials are virtually identical to each other, as would be expected for these two transition metal porphyrins.

In summary, the cyclic voltammetric data in Figures 1 and 2 as well as in Supporting Information, Figure S1 are consistent with two one-electron reductions at the conjugated macrocycle followed by formation of an electroactive phlorin anion as

DOI: 10.1021/acs.inorgchem.5b00067
Inorg. Chem. 2015, 54, 3501−3512

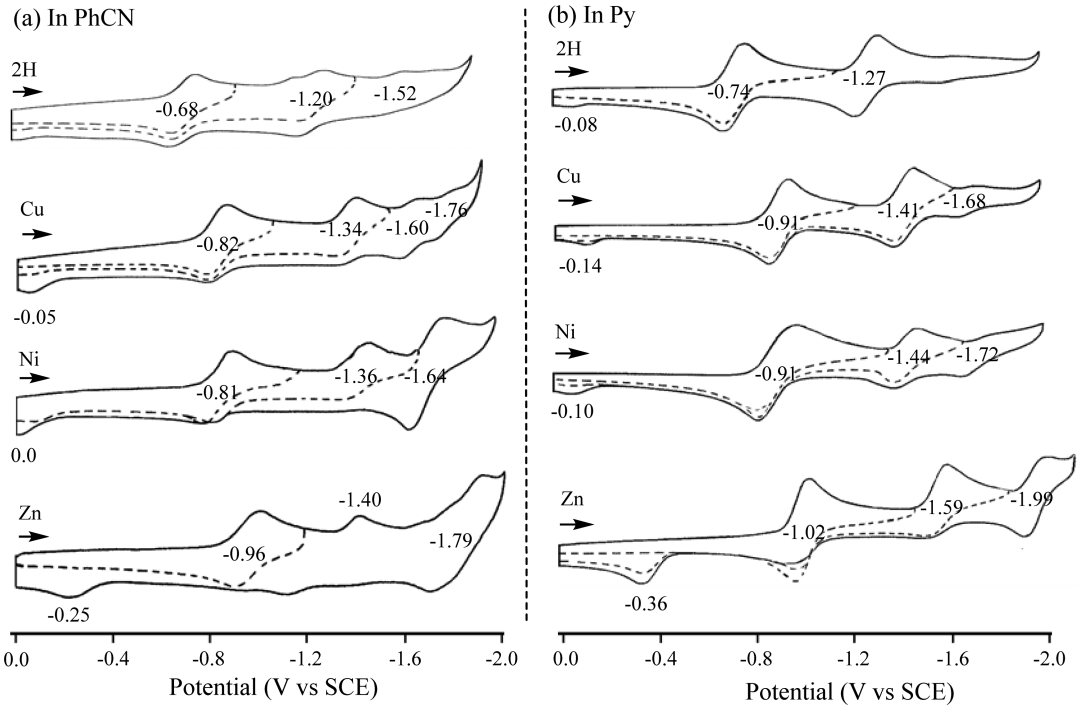

Figure 2. Cyclic voltammograms of investigated compounds $(PhCOOMe)_2(P(O)(OEt)_2)_2PorM$ **2M**, where M = 2H, Cu, Ni, and Zn in (a) PhCN and (b) Py, 0.1 M TBAP.

Scheme 1. Proposed Mechanism for Electron Transfer of Investigated Compounds[a]

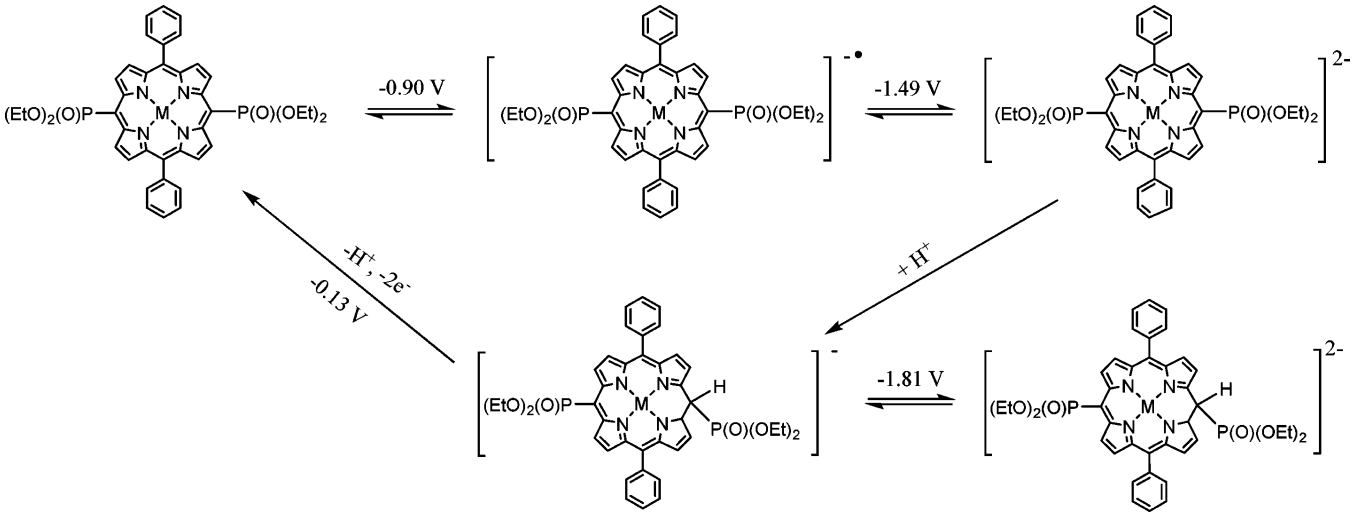

[a]The products in the scheme and the potentials are those for the reduction and reoxidation of $(Ph)_2(P(O)(OEt)_2)_2PorPd$ in PhCN.

shown in Scheme 1, which presents the proposed mechanism. The rationale for this mechanism is based on comparisons with earlier published literature data for the electroreduction of (TPP)Zn[35] and $(TPP)H_2$[34] in DMF as well as by the UV–visible spectroelectrochemistry data described below.

Spectroelectrochemical Monitoring of ***1M*** *Reduction Products, where M = Cu(II), Ni(II), and Pd(II).* Examples of the UV–visible spectral changes obtained during the first two reductions of **1M** in PhCN are shown in Figure 3 for the porphyrins with M = Cu(II), Ni(II), and Pd(II). As presented in Scheme 1, the first one-electron reduction leads to formation of a porphyrin π anion radical, and the spectral changes illustrated in Figure 3a are in each case consistent with this assignment. The final spectrum of the singly reduced porphyrins exhibits a red-shifted and decreased intensity Soret band along with decreased intensity Q bands and characteristic π-anion radical bands in the near-IR region of the spectrum.

Several isosbestic points can be noted in the spectra during conversion of the neutral porphyrin to its radical monoanionic form, and the final spectra for all three porphyrins in Figure 3a are similar to each other. Each singly reduced porphyrin has a band at 431–434 nm in the Soret region of the spectrum and four bands in the visible and near IR region, the three most intense of which are located at ~500, 650, and 820 nm. By way of comparison, the porphyrin π anion radical of (TPP)Pd is characterized by bands at 438, 619, and 869 nm in CH_2Cl_2,

DOI: 10.1021/acs.inorgchem.5b00067
Inorg. Chem. 2015, 54, 3501–3512

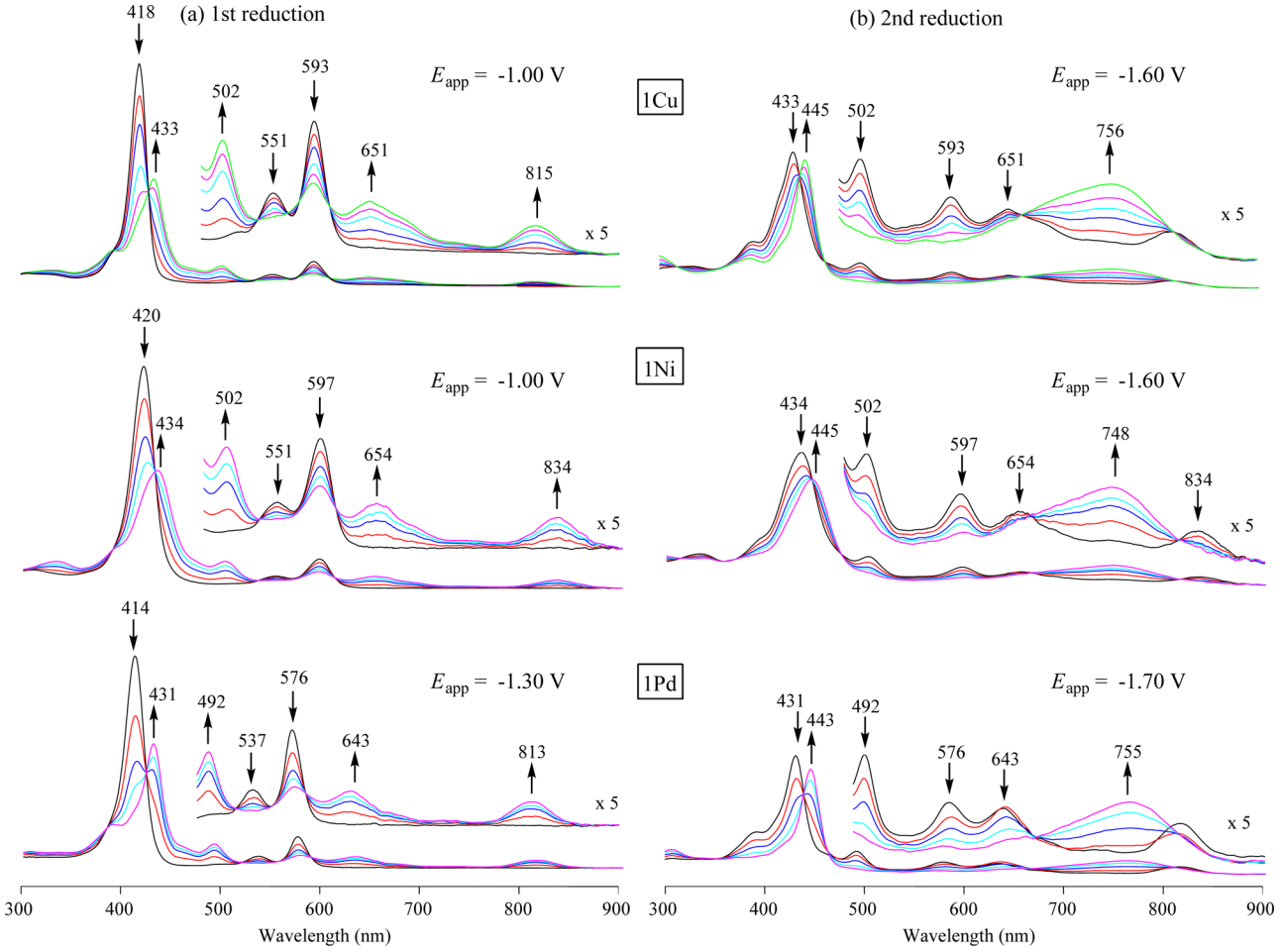

Figure 3. UV−vis spectral changes for solutions of $(Ph)_2(P(O)(OEt)_2)_2$PorM, M = Cu, Ni, and Pd during (a) first reduction and (b) second reduction in PhCN, 0.1 M TBAP.

while the π anion radical of (TPP)Zn in DMF has bands at 457, 725, 806, and 905 nm (unpublished data).

A second controlled potential reduction of the Cu(II), Ni(II), and Pd(II) porphyrins at −1.60 or −1.70 V gave the spectral changes illustrated in Figure 3b. Again, several isosbestic points are observed, and the spectrum of the final reduction products are similar to each other, being characterized by a band in the Soret region at 443−445 nm and broad band at 748−756 nm. These spectra are assigned as belonging to a phlorin anion and are similar to spectra reported for the electrogenerated phlorin dianions of (TPP)Zn and $(TPP)H_2$ in DMF.[34,35]

Electrooxidation. Cyclic voltammograms illustrating oxidation of the phosphoryl porphyrins with redox-inactive central ions are shown in Supporting Information, Figure S2, and a summary of potentials for each oxidation is given in Table 1 (PhCN) and Supporting Information, Table S1 (CH_2Cl_2). Two of the five porphyrins in the **2M** series (Cu^{II} and Zn^{II}) exhibit stepwise one-electron oxidations, and three (H_2, Ni^{II}, and Cd^{II}) are characterized by two overlapping one-electron transfer processes at the same half-wave potential (see Figure S2), while only $\mathbf{1H_2}$ in the case of the **1M** derivatives shows overlapping processes upon conversion of the neutral porphyrin to its dicationic form.

An overlapping of the two porphyrin ring oxidations has often been observed for Ni porphyrins[36−40] and has been explained as resulting from an enhanced axial binding of ClO_4^- from the supporting electrolyte to the doubly oxidized species. This may also be the case for the H_2 and Cd(II) species in the present study where a direct conversion of the neutral porphyrin to its dication radical form occurs in a single step at the same half-wave potential.

Also, as earlier described in the literature, the oxidation of phosphoryl porphyrins is harder than for oxidation of related TPP compounds,[30] with the magnitude of positive shifts in $E_{1/2}$ for the first one-electron abstraction ranging from 230 mV in the case of the Cu(II) porphyrins (0.99 V for (TPP)Cu vs 1.22 V for **1Cu**) to 420 mV in the case of the Cd(II) derivatives (0.72 V for (TPP)Cd vs 1.14 V for **1Cd**). Finally, a third oxidation is observed for **1Ni** and **2Ni**; consistent with the well-known Ni(II)/Ni(III) reactions described in earlier publications.[37−39]

Electrochemistry of 1Co and 2Co. Three one-electron oxidations of **1Co** and **2Co** are observed in PhCN and CH_2Cl_2, while a single oxidation is seen in pyridine, which has a less positive potential window. The first one-electron abstraction is illustrated by the cyclic voltammograms of Figure 4 and corresponds to a Co(II)/Co(III) process, with the next two one-electron oxidations leading to a Co(III) π-cation radical and dication, respectively. The half-wave and/or peak potentials for these processes in the three solvents are listed in Table 3.

The reductive behavior of the cobalt porphyrins differs from that of the other investigated phosphoryl derivatives in that the first two one-electron additions are reversible in PhCN and Py

DOI: 10.1021/acs.inorgchem.5b00067
Inorg. Chem. 2015, 54, 3501−3512

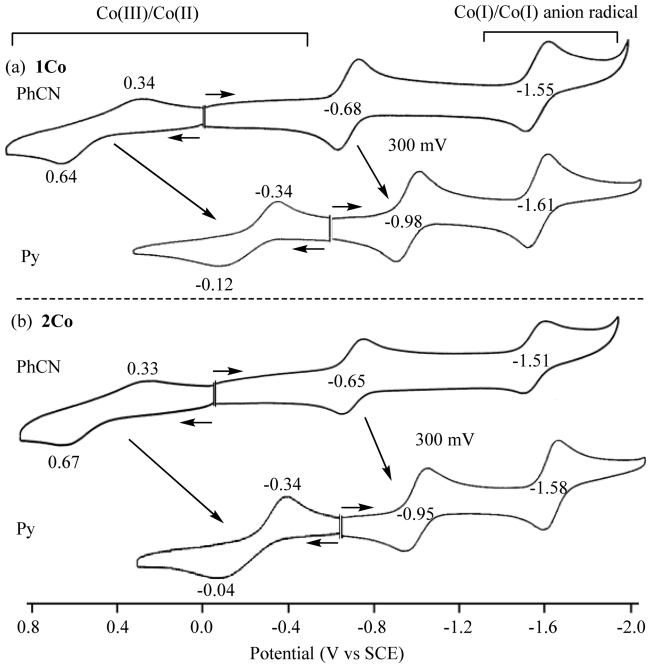

Figure 4. Cyclic voltammograms of (a) $(Ph)_2(P(O)(OEt)_2)_2PorCo$ **1Co** and (b) $(PhCOOMe)_2(P(O)(OEt)_2)_2PorCo$ in **2Co** PhCN and pyridine, 0.1 M TBAP. Scan rate = 0.1 V/s.

with no evidence for formation of a phlorin anion on the electrochemical time scale. The first reduction is also reversible in CH_2Cl_2, and phlorin formation is also not seen in this solvent.

Electrogenerated Co(I) porphyrins are known to rapidly react with CH_2Cl_2[40], and the reversible first reduction in this solvent might suggest electron addition to the conjugated macrocycles of **1Co** and **2Co**. The spectroelectrochemistry data (described below) also suggest formation of Co(II) π anion radical in the first reduction of **1Co** and **2Co**, but this assignment is not consistent with the 300 mV difference in reduction potentials between PhCN and pyridine (see Figure 4), which suggests Co(I) formation in the first step.

The solvent effect of the half-wave potentials in Figure 4 is expected when there is strong binding of two pyridine molecules to Co(III), one pyridine molecule to Co(II), and no pyridine binding to the first reduction product of Co(II).[40] This is consistent with results in the literature for related cobalt porphyrins, which do not bind axial ligands in their Co(I) oxidation state.[40,42−44] The binding of pyridine was examined in the current study by an electrochemically monitored titration of **2Co** with pyridine in PhCN (Figure 5). All axial ligands are

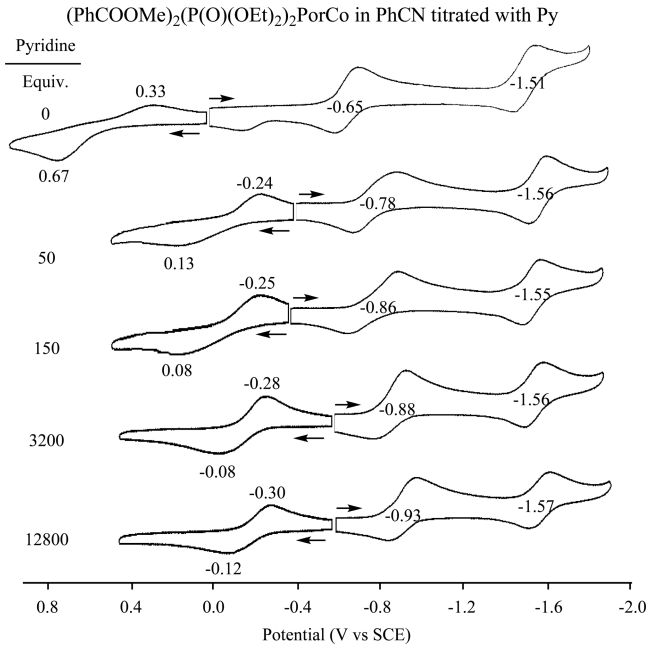

Figure 5. Cyclic voltammograms of $(PhCOOMe)_2(P(O)(OEt)_2)_2PorCo$ **2Co** in PhCN with pyridine, 0.1 M TBAP. Scan rate = 0.1 V/s.

lost upon the first reduction at −0.65 to −0.95 V, and no significant changes in $E_{1/2}$ are seen for the second reduction, which is located at $E_{1/2}$ = −1.55 (**1Co**) or −1.51 V (**2Co**) in PhCN and at −1.61 V (**1Co**) or −1.58 V (**2Co**) in pyridine.

UV−visible spectra for the Co(III), Co(II), and reduced Co(II) forms of the two cobalt porphyrins are shown in Figure 6. The Co(III) product of the first oxidation has bands at 441 and 605 nm, and there are no absorptions between 700 and 900 nm, consistent with electrogeneration of a Co(III) porphyrin with an unoxidized macrocycle. Two ring-centered oxidations of the Co(III) porphyrins are then observed at more positive potentials of +1.37 and +1.49 V (**1Co**) or +1.43 and +1.53 V (**2Co**) (see $E_{1/2}$ values in Table 3).

During the first reduction of **1Co**, the Co(II) porphyrin bands at 416 and 592 nm decrease in intensity as new

Table 3. Half-Wave and Peak Potentials (V vs SCE) of Co(II) Porphyrins in CH_2Cl_2, PhCN, and Py, Containing 0.1 M TBAP

		oxidation				reduction		
		third	second	first	first	first	second	
compound	solvent	$E_{1/2}$	$E_{1/2}$	E_{pa}	E_{pc}	$E_{1/2}$	$E_{1/2}$	ref
$(Ph)_2(P(O)(OEt)_2)_2Por$ **1**	CH_2Cl_2	1.40	1.30	0.58	0.78	−0.67	−1.60[a]	this work (tw)
	PhCN	1.49	1.37	0.64	0.34	−0.68	−1.55	tw
	Py			−0.12	−0.34	−0.98	−1.61	tw
$(PhCOOMe)_2(P(O)(OEt)_2)_2Por$ **2**	CH_2Cl_2	1.43	1.33	0.61	0.81	−0.64	−1.54[a]	tw
	PhCN	1.53	1.43	0.67	0.33	−0.65	−1.51	tw
	Py			−0.04	−0.34	−0.95	−1.58	tw
TPP **3**	CH_2Cl_2	1.16	0.97	0.78		−0.85	−2.05	57
	PhCN	1.39	1.20	0.62	0.38	−0.85	−1.97	58
	Py			−0.21[b]		−1.03		59

[a]Irreversible peak potential at scan rate = 0.1 V/s. [b]$E_{1/2}$ values for reversible Co^{II}/Co^{III} process.

DOI: 10.1021/acs.inorgchem.5b00067
Inorg. Chem. 2015, 54, 3501−3512

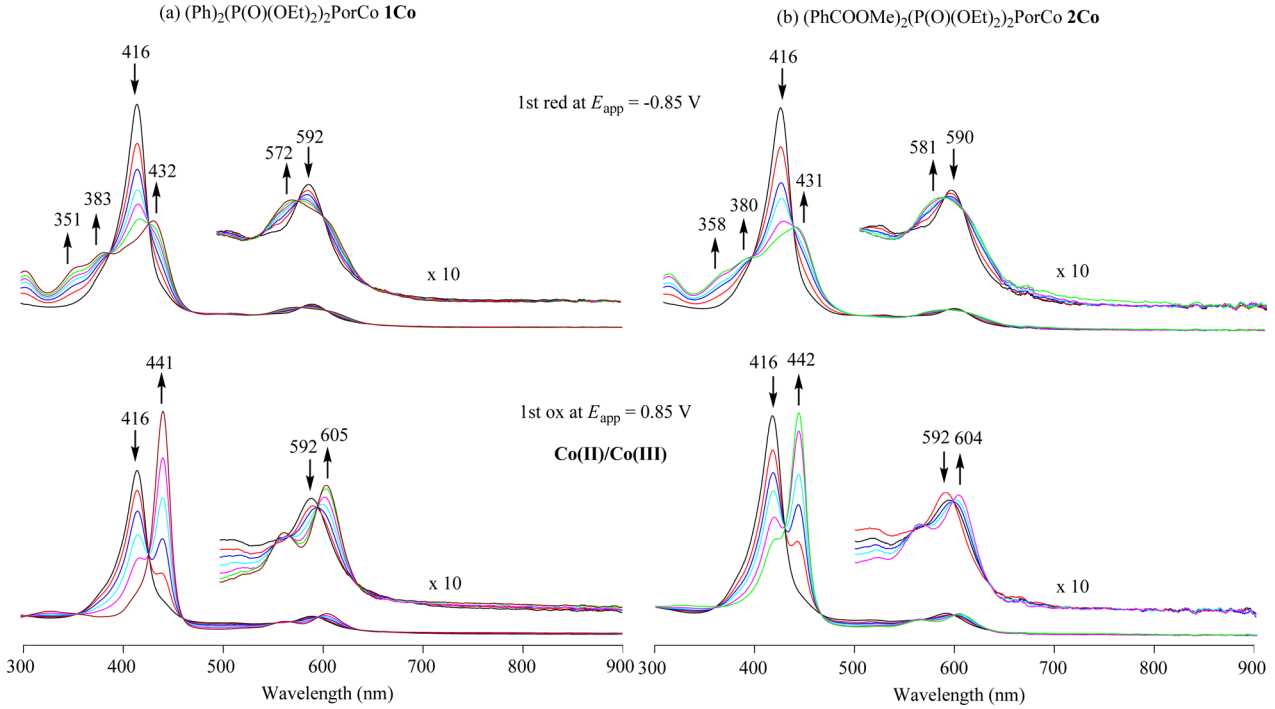

Figure 6. UV−vis spectral changes for solutions of (a) $(Ph)_2(P(O)(OEt)_2)_2PorCo$ and (b) $(PhCOOMe)_2(P(O)(OEt)_2)_2PorCo$ during first reduction and first oxidation in PhCN, 0.1 M TBAP.

porphyrin bands grow in at 351, 383, 432, and 572 nm. As indicated above, these types of UV−visible spectral changes are consistent with formation of a Co(II) π anion radical, rather than formation of a Co(I) porphyrin with an unreduced macrocycle.

In summary, the spectra of the singly reduced species has substantial radical character suggesting a Co(II) π anion radical as the initial product of first one-electron addition, and this is also the conclusion that can be reached by the reversibility of this process in CH_2Cl_2, since the formation of a Co(I) porphyrin would be accompanied by a rapid reaction with the solvent.[44]

The lack of phlorin anion formation after the second reduction of the cobalt derivatives is consistent with a different oxidation state for the doubly reduced porphyrin in the two types of examined compounds, that is, a Co(I) porphyrin π-anion radical in one case and an M(II) porphyrin dianion in the other.

Calculations. The porphyrins studied herein have two different types of *meso* substituents, and therefore the formation of a phlorin from the porphyrin dianion can occur upon protonation at the 5,15 *meso* carbon atoms having phosphoryl groups or at the 10,20 *meso* carbon atoms, with phenyl groups. To determine the most favorable protonation site, calculations for the electronic structure of the porphyrin dianions were performed in terms of analysis of the Fukui function[60−62] ($f^-(\mathbf{r})$) using **1Ni** as an example. This approach was previously applied to explain the reactivity of various metal porphyrinates,[63−65] including their aza-analogues.[66]

Since protonation can be considered as an electrophilic attack of H^+ on the dianion, we investigated the three-dimensional distribution of the $f^-(\mathbf{r})$ function. Within a finite difference approach, this function is defined as a differential change in the electron density $\rho(\mathbf{r})$ induced by a decrease in the number of electrons from N to N − 1 under the conditions of frozen geometry. Therefore, the required Fukui function can be expressed as $f^-(\mathbf{r}) = \rho_N(\mathbf{r}) - \rho_{N-1}(\mathbf{r})$. Areas with positive values of $f^-(\mathbf{r})$ correspond to regions of the molecule that are more sensitive toward electrophilic attack.

To find spatial distribution of $f^-(\mathbf{r})$, density functional theory (DFT) geometrical optimization of the dianion $\mathbf{1Ni}^{2-}$ was performed with the application of SPARTAN'14 software at the B3LYP/6-31G* level. The obtained geometry was used for subsequent single-point calculations of the monoanion $\mathbf{1Ni}^{-}$. These two procedures afforded the distributions of $\rho_N(\mathbf{r})$ and $\rho_{N-1}(\mathbf{r})$, respectively, and their difference map was plotted with the application of CHEMISSIAN 4.33 software (Figure 7).

Analysis of the obtained map (Figure 7) provides evidence that the most reactive atoms of the dianion are located at the 5 and 15 *meso* positions of the molecule. These correspond to the phosphorylated carbon atoms, suggesting that they might be protonated, leading to phlorin anion formation. In contrast, the

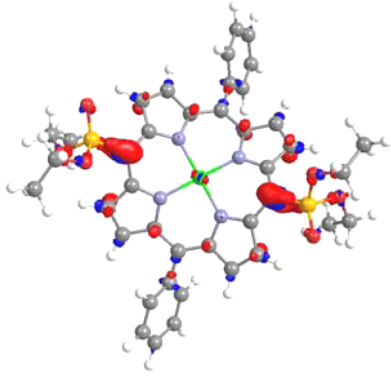

Figure 7. Fukui function $f^-(\mathbf{r})$ plotted for dianion $\mathbf{1Ni}^{2-}$, isovalue -3×10^{-3}; red and blue areas correspond to positive and negative values of $f^-(\mathbf{r})$.

DOI: 10.1021/acs.inorgchem.5b00067
Inorg. Chem. 2015, 54, 3501−3512

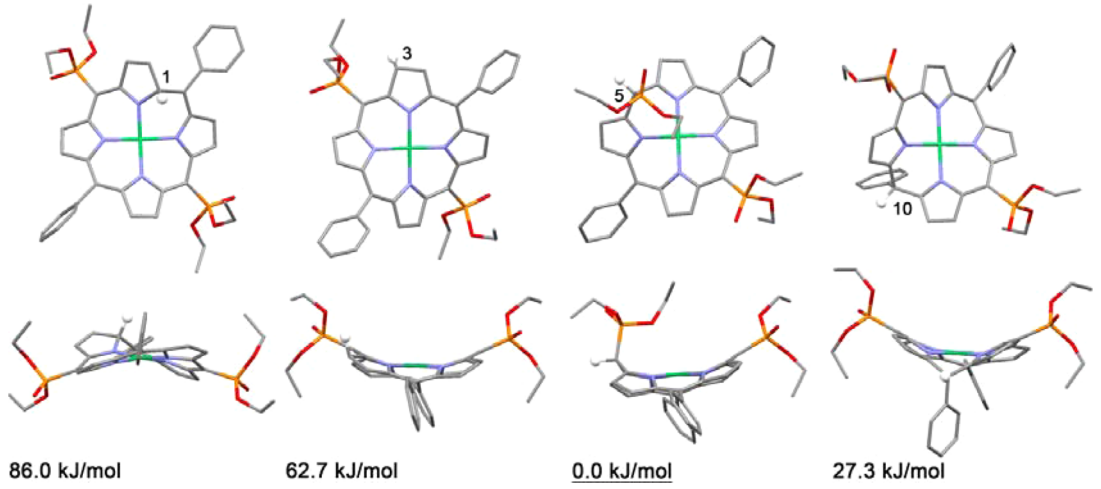

Figure 8. Top and side views of optimized structures of protonated $\mathbf{1Ni}^{2-}$. All hydrogen atoms are omitted except the additional proton at carbon atoms C1, C3, C5, and C10 (shown as a white ball). The energies are given relative to the molecule formed by protonation of C5.

10 and 20 *meso* carbon atoms with phenyl groups have negligibly small values of the $f^{-}(\mathbf{r})$ function, and therefore protonation at these two positions is less favorable. This conclusion is also in agreement with the absence of highest occupied molecular orbital (HOMO) density at C10 and C20.

The Fukui function of $\mathbf{1Ni}^{2-}$ also reveals nonzero values at some of the α- and β-pyrrole atoms (C1 and C3), which could result in susceptibility of these atoms toward protonation. Particularly at the C3 carbon, this could result in formation of a fully conjugated aromatic chlorin-type macrocycle; therefore, such a reaction pathway seemed to be worthy of investigation.

To draw reasonable conclusions about the most likely site of electrophilic attack, four isomeric species, formed by protonation of $\mathbf{1Ni}^{2-}$ at C1, C3, C5, and C10 atoms, were optimized at the B3LYP/6-31G* level of DFT theory to find the most stable isomer. The existence of local minima was verified by normal-mode frequency calculations.

As seen in Figure 8, protonation at the phosphorylated C5 position indeed results in formation of more stable phlorin (by 27.3 kJ/mol) in comparison with the molecule formed upon protonation at the C10 atom. Protonation at the C1 and C3 pyrrole positions results in formation of even less stable species, by 86.0 and 62.7 kJ/mol, respectively, in comparison with the most stable product of C5-protonation.

The DFT-optimized molecular structures of porphyrin **1Ni** and the phlorin anion, obtained by protonation of $\mathbf{1Ni}^{2-}$ at the C5 atom, were used for ZINDO/s calculations of their UV–vis spectra. Calculations revealed that formation of such a phlorin anion should result in a bathochromic shift of the Soret band and the appearance of a band shifted to the red with respect to the Q-band of the starting **1Ni** species (Figure 9). These calculated data are in agreement with the experimental data from spectroelectrochemistry (see Figure 3).

Final Comments. We earlier demonstrated that the shift in reduction potential between (TPP)Zn and a related Zn porphyrin with one β-pyrrole phosphoryl group amounted to ~250 mV.[32] In the current study, we have examined phosphoryl porphyrins with two $P(O)(OEt)_2$ *meso* substituents, and negative shifts in reduction potentials of almost 500 mV are observed as compared to $E_{1/2}$ values for the same redox reactions of the related TPP derivatives.

The positive shift of oxidation potentials due to the electron-withdrawing $P(O)(OEt)_2$ substituents is less than that for

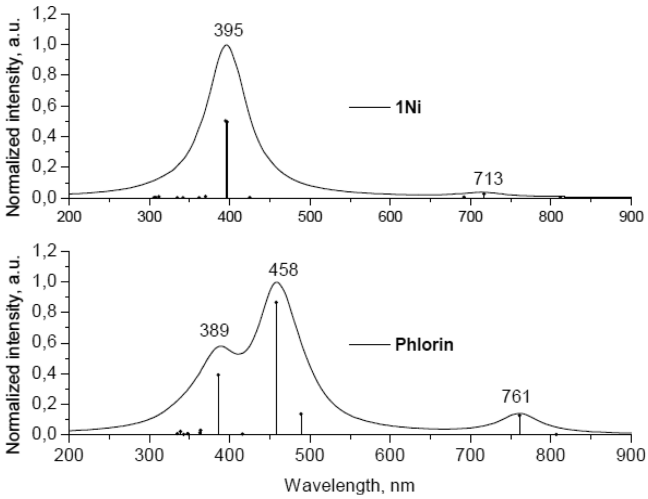

Figure 9. Calculated ZINDO/s spectra of **1Ni** and phlorin, formed by protonation of $\mathbf{1Ni}^{2-}$ at C5 atom. Vertical lines correspond to calculated transitions; the curves correspond to Lorentzian line shape with 30 nm line width.

reduction of the same compounds, and thus the phosphoryl-substituted porphyrins will have a smaller HOMO–LUMO gap than for the related TPP complexes or β-pyrrole monosubstituted phosphoryl porphyrins. The decrease in the HOMO–LUMO gap averages 120 mV upon going from (TPP)M to the diphosphoryl-substituted porphyrins with the same metal ion (see Table 1), and a slightly decreased HOMO–LUMO gap is then observed upon going from compounds in the **1M** series to those in **2M**. This results because the carbomethoxy substituent on two *meso* phenyl groups of **2M** is also electron-withdrawing and shows a larger substituent effect on the reduction potentials than on $E_{1/2}$ values for the oxidation.

Finally, a comment is needed on the site of the first and second reductions for the two examined cobalt porphyrins. The spectra of the singly reduced Co(II) porphyrins have substantial radical anion character, and this conclusion is also suggested by the reversible reductions in CH_2Cl_2 and the lack of reactivity of the singly reduced cobalt porphyrins with this solvent. On the other hand, the large pyridine binding constants for the initial Co(II) porphyrins and the lack of

DOI: 10.1021/acs.inorgchem.5b00067
Inorg. Chem. 2015, 54, 3501–3512

pyridine binding to the singly reduced species is clearly consistent with a Co(II)/Co(I) reaction since Co(I) porphyrins do not bind axial ligands. This could suggest a mixed Co(I) and Co(II) π-anion radical character of the first one-electron reduction product. What is clear is that a porphyrin dianion (and phlorin anion) is not formed after the second reduction of the two cobalt porphyrins, strongly suggesting formation of a Co(I) porphyrin anion radical after the global addition of two electrons.

■ ASSOCIATED CONTENT

Supporting Information

Half-wave potential of investigated compounds, cyclic voltammograms. This material is available free of charge via the Internet at http://pubs.acs.org.

■ AUTHOR INFORMATION

Corresponding Authors

*E-mail: yulia@igic.ras.ru. Phone: (+7) 495 952-25-66. (Y.G.G.)

*E-mail: Roger.Guilard@u-bourgogne.fr. Phone: (+33) (0)3 80-39-61-11. (R.G.)

*E-mail: kkadish@uh.edu. Phone: (+1) 713-743-2740. (K.M.K.)

Notes

The authors declare no competing financial interest.

■ ACKNOWLEDGMENTS

We gratefully acknowledge support from the Robert A. Welch Foundation (K.M.K., Grant No. E-680) and the French-Russian Associated Laboratory "LAMREM" supported by the CNRS and Russian Academy of Sciences, Russian Foundation for Basic Research (Grant No. 12-03-93110).

■ REFERENCES

(1) Alberti, G. *Acc. Chem. Res.* **1978**, *11*, 163−170.

(2) Cao, G.; Hong, H. G.; Mallouk, T. E. *Acc. Chem. Res.* **1992**, *25*, 420−427.

(3) Clearfield, A. *Prog. Inorg. Chem.* **1998**, *47*, 371−510.

(4) Clearfield, A.; Wang, Z. *J. Chem. Soc., Dalton Trans.* **2002**, 2937−2947.

(5) Thompson, M. E. *Chem. Mater.* **1994**, *6*, 1168−1175.

(6) Vermeulen, L. A. *Prog. Inorg. Chem.* **1997**, *44*, 143−166.

(7) Kalyanasundaram, K.; Grätzel, M. *Coord. Chem. Rev.* **1998**, *177*, 347−414.

(8) Maeda, K. *Microporous Mesoporous Mater.* **2004**, *73*, 47−55.

(9) Mutin, P. H.; Guerrero, G.; Vioux, A. *J. Mater. Chem.* **2005**, *15*, 3761−3768.

(10) Shimizu, G. K. H.; Vaidhyanathan, R.; Taylor, J. M. *Chem. Soc. Rev.* **2009**, *38*, 1430−1034.

(11) Gagnon, K. J.; Perry, H. P.; Clearfield, A. *Chem. Rev. (Washington, DC, U.S.)* **2012**, *112*, 1034−1054.

(12) Queffelec, C.; Petit, M.; Janvier, P.; Knight, D. A.; Bujoli, B. *Chem. Rev. (Washington, DC, U.S.)* **2012**, *112*, 3777−3807.

(13) Stern, C.; A, B.-L.; Gorbunova, Y.; Tsivadze, A.; Guilard, R. *Turk. J. Chem.* **2014**, *38*, 980−993.

(14) Lee, J.; Farha, O. K.; Roberts, J.; Scheidt, K. A.; Nguyen, S. T.; Hupp, J. T. *Chem. Soc. Rev.* **2009**, *38*, 1450−1459.

(15) Chou, J.-H.; Kosal, M. E.; Nalwa, H. S.; Rakow, N. A.; Suslick, K. S. In *The Porphyrin Handbook;* Kadish, K. M., Smith, K. M., Guilard, R., Eds.; Academic Press: San Diego, CA, 2000; Vol. *6*, pp 43−131.

(16) Suslick, K. S.; Bhyrappa, P.; Chou, J. H.; Kosal, M. E.; Nakagaki, S.; Smithenry, D. W.; Wilson, S. R. *Acc. Chem. Res.* **2005**, *38*, 283−291.

(17) Zou, C.; Wu, C.-D. *Dalton Trans.* **2012**, *41*, 3879−3888.

(18) Ungashe, S. B.; Wilson, W. L.; Katz, H. E.; Scheller, G. R.; Putvinski, T. M. *J. Am. Chem. Soc.* **1992**, *114*, 8717−8719.

(19) Deniaud, D.; Schollorn, B.; Mansuy, D.; Rouxel, J.; Battioni, P.; Bujoli, B. *Chem. Mater.* **1995**, *7*, 995−1000.

(20) Nixon, C. M.; Le Claire, K.; Odobel, F.; Bujoli, B.; Talham, D. R. *Chem. Mater.* **1999**, *11*, 965−976.

(21) Deniaud, D.; Spyroulias, G. A.; Bartoli, J. F.; Battioni, P.; Mansuy, D.; Pinel, C.; Odobel, F.; Bujoli, B. *New J. Chem.* **1998**, *22*, 901−905.

(22) Rao, P. D.; Littler, B. J.; Geier, G. R.; Lindsey, J. S. *J. Org. Chem.* **2000**, *65*, 1084−1092.

(23) Li, Q. L.; Surthi, S.; Mathur, G.; Gowda, S.; Zhao, Q.; Sorenson, T. A.; Tenent, R. C.; Muthukumaran, K.; Lindsey, J. S.; Misra, V. *Appl. Phys. Lett.* **2004**, *85*, 1829−1831.

(24) Loewe, R. S.; Ambroise, A.; Muthukumaran, K.; Padmaja, K.; Lysenko, A. B.; Mathur, G.; Li, Q. L.; Bocian, D. F.; Misra, V.; Lindsey, J. S. *J. Org. Chem.* **2004**, *69*, 1453−1460.

(25) Bessmertnykh-Lemeune, A. G.; Stern, C.; Gorbunova, Y. G.; Tsivadze, A. Y.; Guilard, R. *Macroheterocycles* **2014**, *7*, 122−132.

(26) Atefi, F.; Arnold, D. P. *J. Porphyrins Phthalocyanines* **2008**, *12*, 801−831.

(27) Vinogradova, E. V.; Enakieva, Y. Y.; Nefedov, S. E.; Birin, K. P.; Tsivadze, A. Y.; Gorbunova, Y. G.; Bessmertnykh Lemeune, A. G.; Stern, C.; Guilard, R. *Chem.—Eur. J.* **2012**, *18*, 15092−15104.

(28) Harvey, P. D.; Stern, C.; Guilard, R. In *Handbook of Porphyrin Science;* Kadish, K. M., Smith, K. M., Guilard, R., Eds.; World Scientific Publishing: Singapore, 2011; Vol. *11*, pp 1−180.

(29) Sinelshchikova, A. A.; Nefedov, S. E.; Enakieva, Y. Y.; Gorbunova, Y. G.; Tsivadze, A. Y.; Kadish, K. M.; Chen, P.; Bessmertnykh-Lemeune, A.; Stern, C.; Guilard, R. *Inorg. Chem.* **2013**, *52*, 999−1008.

(30) Kadish, K. M.; Chen, P.; Enakieva, Y. Y.; Nefedov, S. E.; Gorbunova, Y. G.; Tsivadze, A. Y.; Bessmertnykh-Lemeune, A.; Stern, C.; Guilard, R. *J. Electroanal. Chem.* **2011**, *656*, 61−71.

(31) Matano, Y.; Matsumoto, K.; Terasaka, Y.; Hotta, H.; Araki, Y.; Ito, O.; Shiro, M.; Sasamori, T.; Tokitoh, N.; Imahori, H. *Chem.—Eur. J.* **2007**, *13*, 891−901.

(32) Fang, Y.; Kadish, K. M.; Chen, P.; Gorbunova, Y.; Enakieva, Y.; Tsivadze, A.; Bessmertnykh-Lemeune, A.; Guilard, R. *J. Porphyrins Phthalocyanines* **2013**, *17*, 1035−1045.

(33) Enakieva, Y. Y.; Bessmertnykh, A. G.; Gorbunova, Y. G.; Stern, C.; Rousselin, Y.; Tsivadze, A. Y.; Guilard, R. *Org. Lett.* **2009**, *11*, 3842−3845.

(34) Wilson, G. S.; Peychal-Heiling, G. *Anal. Chem.* **1971**, *43*, 545−550.

(35) Lanese, J. G.; Wilson, G. S. *J. Electrochem. Soc.* **1972**, *119*, 1039−1043.

(36) Fuhrhop, J.-H.; Kadish, K. M.; Davis, D. G. *J. Am. Chem. Soc.* **1973**, *95*, 5140−5147.

(37) Kadish, K. M.; Van Caemelbecke, E.; Boulas, P.; D'Souza, F.; Vogel, E.; Kisters, M.; Medforth, C. J.; Smith, K. M. *Inorg. Chem.* **1993**, *32*, 4177−4178.

(38) Kadish, K. M.; Lin, M.; Van Caemelbecke, E.; De Stefano, G.; Medforth, C. J.; Nurco, D. J.; Nelson, N. Y.; Krattinger, B.; Muzzi, C. M.; Jaquinod, L.; Xu, Y.; Shyr, D. C.; Smith, K. M.; Shelnutt, J. A. *Inorg. Chem.* **2002**, *41*, 6673−6687.

(39) Fang, Y.; Senge, M. O.; Van Caemelbecke, E.; Smith, K. M.; Medforth, C. J.; Zhang, M.; Kadish, K. M. *Inorg. Chem.* **2014**, *53*, 10772−10778.

(40) Kadish, K. M.; Van Caemelbecke, E.; Royal, G. In *The Porphyrin Handbook;* Kadish, K. M., Smith, K. M., Guilard, R., Eds.; Academic Press: New York, 2000; Vol. *8*, p 1−114.

(41) Zubatyuk, R. I.; Sinelshchikova, A. A.; Enakieva, Y. Y.; Gorbunova, Y. G.; Tsivadze, A. Y.; Nefedov, S. E.; Bessmertnykh-Lemeune, A.; Guilard, R.; Shishkin, O. V. *CrystEngComm* **2014**, *16*, 10428−10438.

(42) Kadish, K. M.; Ou, Z.; Tan, X.; Boschi, T.; Monti, D.; Fares, V.; Tagliatesta, P. *J. Chem. Soc., Dalton Trans.* **1999**, 1595−1602.

DOI: 10.1021/acs.inorgchem.5b00067
Inorg. Chem. 2015, 54, 3501−3512

(43) Fukuzumi, S.; Miyamoto, K.; Suenobu, T.; Van Caemelbecke, E.; Kadish, K. M. *J. Am. Chem. Soc.* **1998**, *120*, 2880−2889.
(44) Kadish, K. M.; Han, B. C.; Endo, A. *Inorg. Chem.* **1991**, *30*, 4502−4506.
(45) Ditchfield, R.; Hehre, W. J.; Pople, J. A. *J. Chem. Phys.* **1971**, *54*, 724−728.
(46) Hehre, W. J.; Ditchfield, R.; Pople, J. A. *J. Chem. Phys.* **1972**, *56*, 2257−2261.
(47) Hariharan, P. C.; Pople, J. A. *Theor. Chim. Acta* **1973**, *28*, 213−222.
(48) Francl, M. M.; Pietro, W. J.; Hehre, W. J.; Binkley, J. S.; Gordon, M. S.; DeFrees, D. J.; Pople, J. A. *J. Chem. Phys.* **1982**, *77*, 3654−3665.
(49) Lee, C.; Yang, W.; Parr, R. G. *Phys. Rev. B: Condens. Matter* **1988**, *37*, 785−789.
(50) Becke, A. D. *J. Chem. Phys.* **1993**, *98*, 5648−5652.
(51) Neese, F. *Wiley Interdiscip. Rev.: Comput. Mol. Sci.* **2012**, *2*, 73−78.
(52) Fang, Y.; Bhyrappa, P.; Ou, Z.; Kadish, K. M. *Chem.—Eur. J.* **2014**, *20*, 524−532.
(53) Chang, D.; Malinski, T.; Ulman, A.; Kadish, K. M. *Inorg. Chem.* **1984**, *23*, 817−824.
(54) Wolberg, A.; Manassen, J. *J. Am. Chem. Soc.* **1970**, *92*, 2982−2991.
(55) D'Souza, F.; Zandler, M. E.; Tagliatesta, P.; Ou, Z.; Shao, J.; Van Caemelbecke, E.; Kadish, K. M. *Inorg. Chem.* **1998**, *37*, 4567−4572.
(56) Kadish, K. M.; Shiue, L. R. *Inorg. Chem.* **1982**, *21*, 3623−3630.
(57) Kadish, K. M.; Mu, X. H.; Lin, X. Q. *Inorg. Chem.* **1988**, *27*, 1489−1492.
(58) D'Souza, F.; Villard, A.; Van Caemelbecke, E.; Franzen, M.; Boschi, T.; Tagliatesta, P.; Kadish, K. M. *Inorg. Chem.* **1993**, *32*, 4042−4048.
(59) Walker, F. A.; Beroiz, D.; Kadish, K. M. *J. Am. Chem. Soc.* **1976**, *98*, 3484−3489.
(60) Yang, W.; Mortier, W. J. *J. Am. Chem. Soc.* **1986**, *108*, 5708−5711.
(61) Parr, R. G.; Yang, W. *J. Am. Chem. Soc.* **1984**, *106*, 4049−4050.
(62) Yang, W.; Parr, R. G.; Pucci, R. *J. Chem. Phys.* **1984**, *81*, 2862−2863.
(63) Zhao, L.; Qi, D.; Zhang, L.; Bai, M.; Cai, X. *J. Porphyrins Phthalocyanines* **2012**, *16*, 927−934.
(64) Feng, X.-T.; Yu, J.-G.; Liu, R.-Z.; Lei, M.; Fang, W.-H.; De Proft, F.; Liu, S. *J. Phys. Chem. A* **2010**, *114*, 6342−6349.
(65) Feng, X.-T.; Yu, J.-G.; Lei, M.; Fang, W.-H.; Liu, S. *J. Phys. Chem. B* **2009**, *113*, 13381−13389.
(66) Cardenas-Jiron, G. I. *Int. J. Quantum Chem.* **2003**, *91*, 389−397.

DOI: 10.1021/acs.inorgchem.5b00067
Inorg. Chem. 2015, 54, 3501−3512